

Superconducting Properties of the Fe-Based Layered Superconductor $\text{LaFeAsO}_{0.9}\text{F}_{0.1-\delta}$

G. F. Chen,¹ Z. Li,¹ G. Li,¹ J. Zhou,¹ D. Wu,¹ J. Dong,¹ W. Z. Hu,¹ P. Zheng,¹ Z. J. Chen,¹ H. Q. Yuan,^{2,3} J. Singleton,² J. L. Luo,¹ and N. L. Wang¹

¹Beijing National Laboratory for Condensed Matter Physics, Institute of Physics, Chinese Academy of Sciences, Beijing 100190, China

²National High Magnetic Field Laboratory, MS-E536, Los Alamos National Laboratory, Los Alamos, New Mexico 87545, USA

³Department of Physics, Zhejiang University, Hangzhou 310027, China

(Received 2 March 2008; published 31 July 2008)

We have employed a new route to synthesize single phase F-doped LaOFeAs compound and confirmed the superconductivity above 20 K in this Fe-based system. We show that the new superconductor has a rather high upper critical field of over 50 T. A clear signature of superconducting gap opening below T_c was observed in the far-infrared reflectance spectra, with $2\Delta/kT_c \approx 3.5\text{--}4.2$. Furthermore, we show that the new superconductor has electron-type conducting carriers with a rather low-carrier density.

DOI: 10.1103/PhysRevLett.101.057007

PACS numbers: 74.70.-b, 74.62.Bf, 74.25.Gz

Since the discovery of high-temperature superconductivity in layered cuprates [1], much effort has been made to explore similar phenomenon in other layered transition metal oxides. This has led to the discovery of superconductivity in 4d-transition metal ruthenate Sr_2RuO_4 ($T_c \approx 1.4$ K) [2], and 3d transition metal cobaltate $\text{Na}_x\text{CoO}_2\text{yH}_2\text{O}$ ($x < 0.35$, $y < 1.3$) ($T_c \approx 4$ K) [3]. Recently, Kamihara *et al.* found that the iron- or nickel-based layered compounds LaOMP ($M = \text{Fe}, \text{Ni}$) exhibit superconductivity with transition temperatures $T_c \approx 3 \sim 5$ K [4,5]. The structure contains alternate stacking of La_2O_2 and $M_2\text{P}_2$ layers along the c axis, with the M ion locating in the center of the P tetrahedron. This discovery came as a surprise for the scientific community since the superconductivity comes from the Fe or Ni 3d electrons, while in the usual case the 3d electrons in Fe- or Ni-based compounds tend to form local moments and to develop magnetic orderings at low temperature. Very recently, the same group reported that, with the replacement of P by As and partial substitution of O^{2-} by F^- in the Fe-based compound to yield $\text{LaFeAs}(\text{O}_{1-x}\text{F}_x)$, its T_c could reach as high as 26 K at 5–10 at. % F doping [6]. This is an exciting event since, except for the high-temperature superconductivity in copper oxides, the T_c in this system has already become the highest among layered transition metal-based compounds. This remarkable discovery not only opens up new possibilities for exploring novel superconducting compounds with potentially higher T_c , but also offers opportunity to study the origin of superconductivity from transition metal d -band electrons, which is expected to shed new light on the mechanism of high-temperature superconductivity in cuprates.

We have employed a new route to synthesize single phase F-doped LaFeAsO compound and confirmed the superconductivity above 20 K in this system. In this work, we present the fundamental superconducting properties of this system by performing resistivity, magnetic susceptibility, Hall effect, and optical measurements. We

show that the new superconductor has a rather high upper critical field of over 50 T. We observed a clear signature of superconducting gap formation below T_c with an expected BCS gap amplitude. Besides, the compound has electron-type conducting carriers with a rather low-carrier density.

The polycrystalline samples were prepared by the solid state reaction using LaAs, Fe_2O_3 , Fe, and LaF_3 as starting materials. Different from the synthesis method reported by Kamihara *et al.* [6], we use Fe_2O_3 as a source of oxygen instead of La_2O_3 due to the high stability of Lanthanum oxide. Lanthanum arsenide (LaAs) was obtained by reacting La chips and As pieces at 500 °C for 12 h then at 850 °C for 2 h. Mixtures of four components were ground thoroughly and cold-pressed into pellets. The pellets were placed into Ta crucible and sealed in quartz tube under argon atmosphere. They were then annealed for 50 h at a temperature of 1150 °C.

The phase purity was checked by a powder x-ray diffraction method using Cu $K\alpha$ radiation at room temperature. As shown in Fig. 1, the powder x-ray diffraction pattern of the resultant is well indexed on the basis of tetragonal ZrCuSiAs-type structure with the space group $P4/nmm$ [7]. No obvious foreign phase was detected,

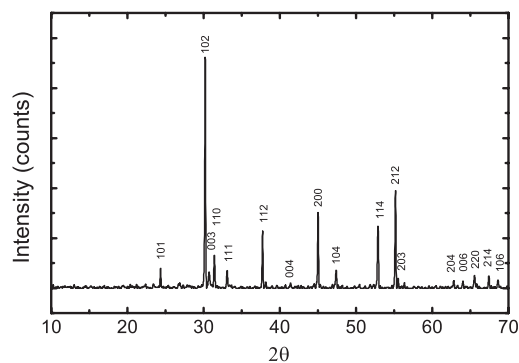


FIG. 1. X-ray powder diffraction pattern of $\text{LaFeAsO}_{0.9}\text{F}_{0.1-\delta}$.

ensuring the proposed treatment was successful to obtain a single phase $\text{LaFeAsO}_{0.9}\text{F}_{0.1-\delta}$ sample. In the present study we adopt $0.1 - \delta$ for the fluorine concentration in the sample because we cannot evaluate possible evaporation loss of the F^- component during the high-temperature annealing. The lattice parameters of $\text{LaFeAsO}_{0.9}\text{F}_{0.1-\delta}$ are $a = 0.4024$ nm and $c = 0.8717$ nm, respectively, obtained by a least-squares fit to the experimental data. Compared to the undoped phase LaFeAsO [7], the unit cell volume was reduced $\sim 1\%$ upon $\sim 10\%$ F doping, indicating a successful chemical substitution.

The electrical resistivity was measured by means of a standard four-probe method in a Quantum Design physical property measurement system (PPMS). The T dependence of the resistivity at zero magnetic field is shown in Fig. 2. With decreasing temperature, the resistivity decreases monotonously and a rapid drop was observed starting at about 26 K, indicating the onset of superconductivity. To confirm the superconductivity, we measured the ac magnetic susceptibility with a modulation field of 10 Oe and 333 Hz below 30 K on the same sample. The lower inset of Fig. 2 shows the temperature dependence of the real part of ac magnetic susceptibility. We clearly observed the appearance of superconducting diamagnetism at 20 K. The broadening of the magnetic transition reflects certain inhomogeneity in the polycrystalline sample.

The upper critical field H_{c2} is one of the important parameters to characterize superconductivity. To get information about H_{c2} of $\text{LaFeAsO}_{0.9}\text{F}_{0.1-\delta}$ sample, we measured the electrical resistivity under selected magnetic fields up to 14 T in PPMS, as shown in the upper inset of Fig. 2. With increasing the field, the transition temperature T_c shifts to lower temperature and the transition width gradually becomes broader, similar to the high T_c cuprate superconductors [8,9], suggesting the strong anisotropy of the critical field, as expected from the two-dimensional electronic structure [10]. As the T_c was suppressed by only several kelvins under a field of 14 T, the $H_{c2}(0)$ value is obviously very high.

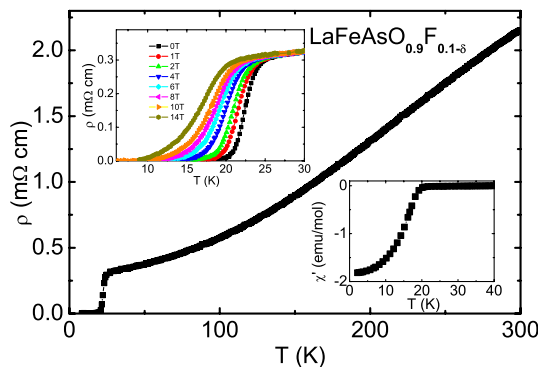


FIG. 2 (color online). The electrical resistivity vs temperature of $\text{LaFeAsO}_{0.9}\text{F}_{0.1-\delta}$. Lower inset: temperature dependence of the real part of ac magnetic susceptibility. Upper inset: the resistivity vs temperature curves at selected magnetic fields.

It is highly desirable to have more direct information about the upper critical field. For this purpose, we determined H_{c2} , in pulsed magnetic fields up to 55 T at Los Alamos, using a tunnel-diode oscillator (TDO) technique in which two small counter-wound coils form the inductance of a resonant circuit [11]. The resonant frequency, in our case about 31 MHz, can depend on both the skin-depth (or, in the superconducting state, the penetration depth) and the differential magnetic susceptibility of the sample. A piece of thin sample (about $1.3 \times 0.75 \times 0.15$ mm³) was inserted in the coils, which were immersed in ³He liquid or ³He exchange gas, temperatures being measured with a Cernox thermometer 5 mm away from the sample.

Figure 3 shows the field dependence of the TDO frequencies at $T = 25, 15, 10, 4, 0.55$ K, respectively. Superconductivity, with a relatively broad transition as evidenced in the figure, is eventually suppressed by applying a high magnetic field. In order to determine the upper critical fields H_{c2} , the TDO frequencies $f(H)$ were first fitted with suitable polynomial expressions, then one calculates the derivatives of these fitted functions with regard to magnetic field. As shown in the inset (a), the curvature of derivative df/dH clearly follows different slopes on the two sides of the critical field H_{c2} , with H_{c2} being determined by the cross point of the extended slopes as indicated by the straight lines. Inset (b) shows the extracted critical magnetic field vs temperature phase diagram. We found that the zero-temperature $H_{c2}(0)$ is over 50 T. In the figure, we also include data points of H_{c2} determined from the resistivity measurement under dc magnetic field below 14 T, where $T_c(H)$ is defined as a temperature at which the resistivity falls to half of the normal state value (middle

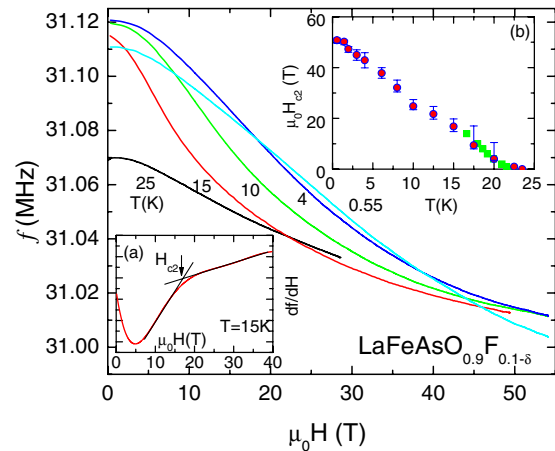


FIG. 3 (color online). The field dependence of the TDO frequencies at $T = 25, 15, 10, 4, 0.55$ K, respectively. Inset (a): curve for the derivative of TDO frequency with respect to field, df/dH , at 15 K. The critical field is determined by the cross point of the two slopes in the derivative curve as indicated by the straight lines. Inset (b): critical field vs temperature phase diagram. The data points obtained from the midpoint of resistivity drop at T_c are also include (green square symbol).

transition). One can see that the two methods give very consistent results of H_{c2} . The H_{c2} vs T curve has a slight upward curvature (see Note added).

The superconducting energy gap is another important parameter for a superconductor. To obtain the gap information below the superconducting transition, we measured optical reflectance across T_c in the far-infrared region on a polished sample in a Bruker 113v spectrometer. A 2.5 mm thick silicon was used as the beam splitter. The thick silicon beam splitter has superior long-wavelength performance, enabling us to obtain enough signal down to very far-infrared region. Figure 4 shows the reflectance curves between 16 and 300 cm^{-1} at different temperatures. The low frequency reflectance $R(\omega)$ increases with decreasing temperature, which is a typical metallic response. A reasonable estimation for the maximum value of superconducting gap could be taken from a comparison of the reflectance at $T \ll T_c$ and $T \approx T_c$. Because the sharp transition in magnetic susceptibility appears at 20 K, little difference could be found for the reflectance curves at 20 and 29 K. However, for the $R(\omega)$ at 8 K, an abrupt increase below 50 \sim 60 cm^{-1} as indicated by an arrow in the figure could be seen as compared with curves at 20 and 29 K. This feature is very similar to other superconducting compounds below T_c [12–14], and apparently could be attributed to the gap formation in the density of state. The superconducting gap is therefore estimated to be close to $2\Delta \approx 50 \sim 60 \text{ cm}^{-1}$. This yields a $2\Delta/kT_c$ ratio of 3.5–4.2, being in good agreement with the expected value within BCS theory.

For an s -wave superconductor without nodes, the reflectance for $T \ll T_c$ approaches to unity abruptly below the gap energy [13]. This is not the case for the present sample, instead $R(\omega)$ changes in a way very similar to high- T_c superconductor, for example, $\text{Pr}_{1.85}\text{Ce}_{0.15}\text{CuO}_4$ [12]. This may indicate the existence of a significant density of states within the gap, or the pairing symmetry is not s wave. However, since the sample we measured is a polycrystalline sample, conclusive information on the gap symmetry

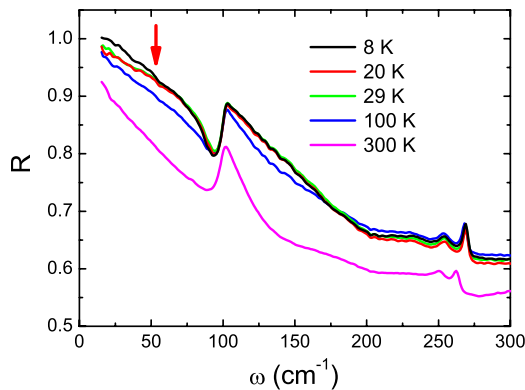


FIG. 4 (color online). The far-infrared reflectance spectra at different temperatures. The arrow indicates the frequency below which a steep rise appears for the case of $T \ll T_c$.

could not be drawn at this stage. For the same reason, we also would not address other features appearing in the reflectance curves, such as the pronounced phonon structures, and the fast decreasing of $R(\omega)$ with increasing frequency.

To get more information about the conducting carriers, we measured the Hall coefficient in the normal state using a five-probe technique in PPMS. Figure 5 shows the Hall coefficient data between 30 and 200 K. The inset shows the five-leads measurement configuration, and the verification of the Hall voltage driven by magnetic field where a linear dependence of the transverse voltage on the applied magnetic field is observed up to 5 T at 30 K. Two sets of data were presented in the main panel. The red squares are Hall coefficient data measured by scanning magnetic field at fixed temperature, while the solid black curve is R_H determined from two separate temperature scans under fixed applied magnetic field at ± 5 T, respectively. They show a rather good match. The experiment indicates that the Hall voltage is negative, suggesting electron-type conducting carriers in this compound.

An interesting result here is that the Hall coefficient is T dependent. The absolute R_H value increases with decreasing T . Large T -dependence of R_H was also observed in high-temperature superconductors, and was regarded as one of the exotic properties [15]. For a metal, the T -dependent R_H is often explained by the multiband effect. When the carrier scattering rates change with temperature at different rates for different bands, R_H can become strongly T dependent [15]. Indeed, a recent band structure calculation for LaFePO indicates that all the five Fe d -orbital energy levels are not fully occupied; they cross the Fermi level E_F , leading to five Fermi surfaces [10]. So it is possible that the T dependence of R_H comes from the multiband effect. Alternatively, the T dependence of R_H could also be caused by a magnetic skew scattering mecha-

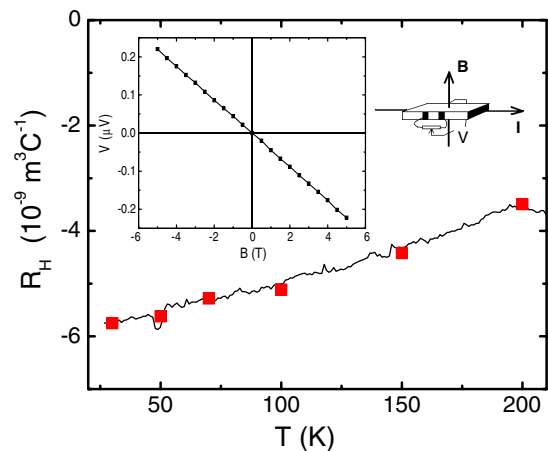


FIG. 5 (color online). The Hall coefficient vs temperature for the sample. The inset shows that the transverse voltage measured at $T = 30$ K is proportional to the applied magnetic field. The five-leads measurement configuration is also shown.

nism: the scattering of conduction electrons from local moments is asymmetric due to spin-orbital coupling [15]. Magnetic skew scattering has been observed in various materials with the presence of magnetic moments. As the compound contains Fe element, there exists chance for the presence of Fe^{2+} impurities with local moments, then the skew scattering mechanism might also work here. At present, we could not distinguish between the above different possibilities. Because the Hall coefficient changes with temperature, it is not easy to determine the carrier number precisely from the measurement result. A rough estimation simply based on the relation $R_H = 1/ne$ indicates that the carrier density is rather low, for example, at 200 K, the carrier density is $1.8 \times 10^{21} \text{ cm}^{-3}$, being similar to the high- T_c cuprates [15].

Before concluding, we would like to address the origin of the conduction carriers and possible constraint from the experimental data. From the balance of the valence states in LaFeAsO or LaFePO , La^{3+} , O^{2-} , and P^{3-} are expected to have closed shells, or to form fully occupied orbitals, only Fe^{2+} has 6 electrons in $3d$ orbitals. The Fe^{2+} ion locates at the center of the P^{3-} tetrahedral. In such a crystal field, the $3d$ energy levels split into the lower e_g ($d_{x^2-y^2}$, d_{z^2}) and the upper t_{2g} (d_{xy} , d_{yz} , d_{xz}). In crystal structure, the P^{3-} tetrahedral was suppressed a bit along the c axis [4], leading to the further splitting of e_g and t_{2g} (the d_{z^2} orbital is pushed to high energy, on the contrary, the $d_{x^2-y^2}$ and d_{xy} levels are slightly lowered). According to the band structure calculation for LaFePO [10], all those Fe $3d$ orbitals are not fully filled, leading to five Fermi surfaces (without forming local moment), we can expect that the Hund's rule coupling is rather weak in comparison with bandwidth broadening in such systems. F^- doping into the structure should further increase the electron number. However, if all the Fe $3d$ electrons contribute to the conduction and superconductivity, we would expect a rather high carrier density. The small carrier density in our measurement result highly suggests that not all Fe $3d$ electrons contribute to the conduction. Apparently, further experimental and theoretical studies are called on to solve the inconsistency, and to understand the superconducting mechanism in those compounds.

To summarize, we have made an intensive study of superconducting properties on F^- doped sample $\text{LaFeAsO}_{0.9}\text{F}_{0.1-\delta}$. We found the onset of superconductivity occurs close to ~ 26 K. The main magnetic transition appears near 20 K. We found a rather high upper critical field of over 50 T and a clear signature of superconducting energy gap opening below T_c . A rather low-carrier density was revealed from the Hall effect measurement, with the conducting carriers being of electron-type.

We acknowledge very helpful discussions with T. Xiang and L. Yu. This work is supported by the National Science Foundation of China, the Chinese Academy of Sciences, the 973 project of the Ministry of Science and Technology of China and the PCSIRT of the Ministry of Education of China. Work at NHMFL is performed under the auspices of the National Science Foundation, DOE, and the State of Florida.

Note added.—Very recently, Hunte *et al.* [16] reported measurement of H_{c2} under dc magnetic field up to 45 T and revealed an upward curvature at low temperature, which they ascribed to the two-band effects.

-
- [1] J.G. Bednorz and K.A. Muller, Z. Phys. B **64**, 189 (1986).
 - [2] Y. Maeno, H. Hashimoto, K. Yoshida, S. Nishizaki, T. Fujita, J.G. Bednorz, and F. Lichtenberg, Nature (London) **372**, 532 (1994).
 - [3] K. Takada, H. Sakurai, E. Takayama-Muromachi, F. Izumi, R.A. Dilanian, and T. Sasaki, Nature (London) **422**, 53 (2003).
 - [4] Y. Kamihara, H. Hiramatsu, M. Hirano, R. Kawamura, H. Yanagi, T. Kamiya, and H. Hosono, J. Am. Chem. Soc. **128**, 10 012 (2006).
 - [5] T. Watanabe, H. Yanagi, T. Kamiya, Y. Kamihara, H. Hiramatsu, M. Hirano, and H. Hosono, Inorg. Chem. **46**, 7719 (2007).
 - [6] Y. Kamihara, T. Watanabe, M. Hirano, and H. Hosono, J. Am. Chem. Soc. **130**, 3296 (2008).
 - [7] P. Quebe, L.J. Terbüchte, and W. Jeitschko, J. Alloys Compd. **302**, 70 (2000).
 - [8] T.T.M. Palstra, B. Batlogg, L.F. Schneemeyer, and J.V. Waszczak, Phys. Rev. Lett. **61**, 1662 (1988).
 - [9] U. Welp, W.K. Kwok, G.W. Crabtree, K.G. Vandervoort, and J.Z. Liu, Phys. Rev. Lett. **62**, 1908 (1989).
 - [10] S. Lebgue, Phys. Rev. B **75**, 035110 (2007).
 - [11] E.A. Yelland, J. Singleton, C.H. Mielke, N. Harrison, F.F. Balakirev, B. Dabrowski, and J.R. Cooper, Phys. Rev. Lett. **100**, 047003 (2008).
 - [12] C.C. Homes, R.P.S.M. Lobo, P. Fournier, A. Zimmers, and R.L. Greene, Phys. Rev. B **74**, 214515 (2006).
 - [13] M. Ortolani, S. Lupi, L. Baldassarre, U. Schade, P. Calvani, Y. Takano, M. Nagao, T. Takenouchi, and H. Kawarada, Phys. Rev. Lett. **97**, 097002 (2006).
 - [14] S. Lupi, L. Baldassarre, M. Ortolani, C. Mirri, U. Schade, R. Sopracase, T. Tamegai, R. Fittipaldi, A. Vechione, and P. Calvani, arXiv:0710.2259.
 - [15] see, for example, N.P. Ong, in *Physical Properties of High Temperature Superconductors II*, editor by D.M. Ginsberg (World Scientific, Singapore, 1990), p. 459.
 - [16] F. Hunte, J. Jaroszynski, A. Gurevich, D.C. Larbalestier, R. Jin, A.S. Sefat, M.A. McGuire, B.C. Sales, D.K. Christen, and D. Mandrus, Nature (London) **453**, 903 (2008).